JOURNAL OF PROPULSION AND POWER
Vol. 18, No. 6, November–December 2002

Hydrogen Peroxide Decomposition on Various Supported Catalysts Effect of Stabilizers

Laurence Pirault-Roy,* Charles Kappenstein,† Maurice Guérin,‡ and Rachel Eloirdi§
Université de Poitiers et Centre National de la Recherche Scientifique, F-86022 Poitiers, France
and
Nicolas Pillet¶
Centre National d'Etudes Spatiales, Toulouse, France F-31401

The decomposition of hydrogen peroxide (H_2O_2) has been studied on various catalysts (platinum supported on silica; silver, iridium, platinum–tin or manganese oxides supported on alumina). The experiments were performed using two reactors: 1) a conventional constant pressure reactor for the determination of the volume increase vs time using diluted H_2O_2 solutions; 2) a constant volume reactor to measure the pressure increase using more concentrated solutions. The first reactor leads to the determination of the kinetic order of the reaction, to the comparison of the activities of the different samples, and to the characterization of the influence of some stabilizers of H_2O_2 solutions on the catalytic activity. Two kinetic orders were found, depending on the catalyst: a zero order and a first order. The shape of the catalysts samples is an important parameter, with powders always being more reactive than grains and pellets. The catalyst activities are sorted as follows: $Pt–Sn/Al_2O_3 < Ir/Al_2O_3 < Pt/SiO_2 < MnO_x/Al_2O_3 < Ag/Al_2O_3$. The presence of pyrophosphate stabilizer leads to a loss of activity mainly as a result of passivation in the case of MnO_x-supported samples, whereas the presence of stannate increases slightly the activity of silver and displays no influence on manganese samples.

Introduction

THE replacement of hydrazine[1] (N_2H_4) and/or NTO (N_2O_4) by "green propellants" is of current interest to overcome the disadvantages of hydrazine due to its toxicity and to safe handling regulations. Different new formulations are proposed[2] and are presently under investigation in different laboratories. They can be sorted into two types.

The first type comprises aqueous blended solutions containing an oxidant and a reductant or fuel. Three oxidants have been proposed: hydroxylammonium nitrate (HAN) associated with triethanolammonium nitrate (TEAN),[3] glycine, methanol,[4] and ethanol[3,5,6]; ammonium dinitramide (ADN) associated with glycerol[7]; or hydrazinium nitroformate (HNF) fuel-based mixture.[8]

The second type comprises concentrated hydrogen peroxide solutions alone[9–11] associated with polyethylene or other solid fuels in hybrid engines[12–15] or associated with suitable liquid fuels.

Each monopropellant has to be associated with a catalyst that shows the highest activity and the best stability in operating conditions. In such cases, the onset temperature of the catalytic decomposition must be as low as possible to avoid preheating treatments that are essential for high-temperatures decomposition.

The aqueous propellants containing oxidizer and reductant species (redox propellants) are relatively stable for long-term storage or during handling, but need high preheating temperatures of the catalytic bed (up to 450°C), to shorten the ignition delay and to avoid the formation of solid carbonaceous products.

On the other hand, the decomposition of H_2O_2 can be triggered at low temperature, but the long-term stability of the aqueous concentrated solutions generally requires the presence of stabilizing agents. Despite the kinetic stability of pure H_2O_2 solutions, slow decomposition rates are observed and can be attributed to the presence of impurity traces displaying a catalytic effect or a catalytic reaction with the storage container. Therefore, the solutions are stabilized, that is, the impurities are deactivated, by the addition of small amounts of the following stabilizers.[16–18]

1) Disodium dihydrogenodiphosphate (or sodium pyrophosphate) $Na_2H_2P_2O_7$ [Chemical Abstract Service Registry Number (CAS RN) 7758-16-9] can complex the metallic cations and inhibit their catalytic behavior.

2) Sodium stannate trihydrate $Na_2SnO_3.3H_2O$ or $Na_2Sn(OH)_6$ (CAS RN 12058-66-1) forms tin oxide or hydroxide colloidal particles. These particles coat the impurities and, thus, hinder the contact with the solution.

3) Nitrate ions can inhibit the corrosion of aluminum drums due to the presence of Cl^- ions.

In the present paper, we focus on the decomposition of hydrogen peroxide with two main objectives: 1) determination of the order of the reaction for different catalysts and 2) study of the influence of stabilizing agents on the catalytic activity. To study the first stages of decomposition of H_2O_2 in particular and to compare easily the different catalysts tested, we made use of two specific apparatus: a constant pressure reactor and a constant volume batch reactor.

Experimental Part

Reactors

The first reactor used was designed to work at constant pressure and temperature. It can measure evolved oxygen volumes up to 60 ml (shown in Fig. 1). The aqueous diluted H_2O_2 solution (10 ml) is in excess in the reactor, and the catalyst (10–400 mg) is added rapidly by turning the sample tube to start the decomposition. The internal pressure of the reactor is kept constant by displacing water from both burettes. The volume of displaced water gives directly

Received 3 January 2002; revision received 11 July 2002; accepted for publication 18 July 2002.

*Doctor, Laboratoire de Catalyse en Chimie Organique.
†Professor, Laboratoire de Catalyse en Chimie Organique, Unité Mixte de Recherche 6503, Catalyse par les Métaux, 40 Avenue du Recteur Pineau; Charles. Kappenstein@univ-poitiers.fr. Member AIAA.
‡Professor, Laboratoire de Catalyse en Chimie Organique.
§Doctor, Laboratoire de Catalyse en Chimie Organique.
¶Dipl.-Ing., Propulsion and Pyrotechnic Department.

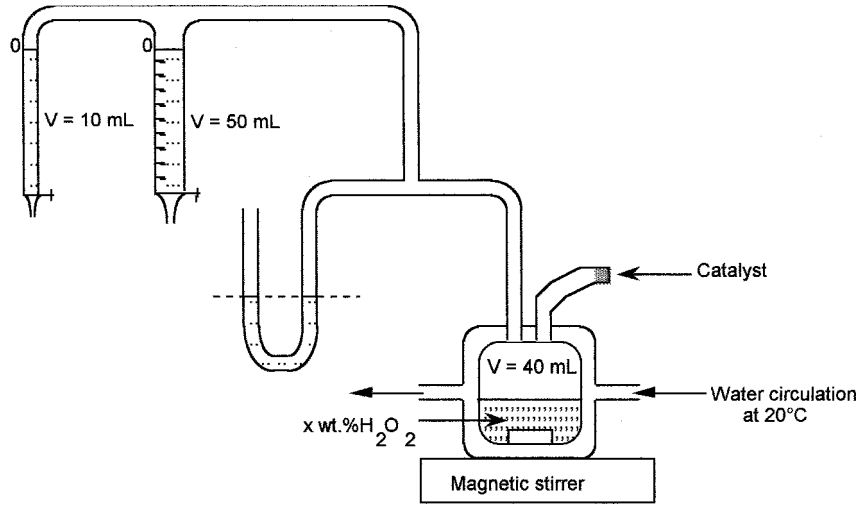

Fig. 1 Scheme of the constant pressure reactor for measurements of oxygen volumes released from H_2O_2 catalytic decomposition vs time.

the volume of evolved oxygen (if we neglect the very small increase in oxygen solubility). A magnetic stirrer provides constant stirring of the reactants. During the experiments, the temperature of the reactants is kept constant by a temperature-regulated water flow in the double wall reactor. The (H_2O_2)/(active center) molar ratios range from 50 (for Ir/Al_2O_3) to 665 (for $Pt–Sn/Al_2O_3$), calculated on the basis of the initial weights.

The second reactor is a constant volume batch reactor (168 ml) with operating pressure between vacuum and 2 bar 1 bar = 0.1 MPa. It has been described and presented previously.[19,20] It is equipped by three temperature gauges, K thermocouples with low time response (0.1 s) located near the heating element, the catalyst, and the inside of the reactor atmosphere, and one pressure gauge (time response less than 1 ms in the range 0–2 bar), all connected to the computer through an interface. The catalyst (100–200 mg) can be heated with a fixed slope or preheated at a defined temperature. The monopropellant is added through a Hamilton microsyringe (100 μl). Between two monopropellant injections, the decomposition products can be quickly evacuated through the vacuum line up to 10^{-2} mbar. Note that, after a H_2O_2 addition, the temperature increase is limited to about 100°C because the heat evolved is not sufficient to vaporize all of the water. In a few seconds, the temperature drops to room temperature due to the important heat transfer to the walls of the reactor. For the batch reactor, the (H_2O_2)/(active center) molar ratios are in the range of 14–30, based on the initial weights.

Monopropellant

For tests in the batch constant volume reactor, the monopropellant is hydrogen peroxide H_2O_2, 30 and 50 wt% (Prolabo, France), with the following impurities: heavy metals, 5 ppm; Cl, 5 ppm; Ca, 5 ppm; Fe, 5 ppm; Mg, 5 ppm; and N, total 20 ppm.

It is diluted to the range 1.6–4.7 wt% for tests in the constant pressure reactor.

Catalysts

The catalysts are as follows: 1) Ag, from Alfa–Johnson Mathey, 99.99% purity, and 10–20 mesh; 2) Ag/Al_2O_3, from Strem Chemicals, pellets, 3.5–4 wt% Ag, S_{BET} 8 $m^2 \cdot g^{-1}$; 3) Pt/SiO_2 grains, 6.3 wt% Pt, and 60% dispersion[21]; 4) Ir/Al_2O_3, from the Snecma Company, France, grains, 36 wt% Ir, and 20% dispersion; 5) $Pt–Sn/Al_2O_3$, powder, 1 wt% Pt, 0.61 wt% Sn; Pt dispersion 4% (Refs. 22 and 23); and 6) MnO_x/Al_2O_3, powder, prepared by impregnation of the carrier with $HMnO_4$ followed by calcination at 150°C during 5 h, no x-ray detectable manganese oxide bulk phase,[24] 1.6 wt% Mn, and S_{BET} 54 $m^2 \cdot g^{-1}$.

For some experiments, the pellets or grains have been ground to a powder.

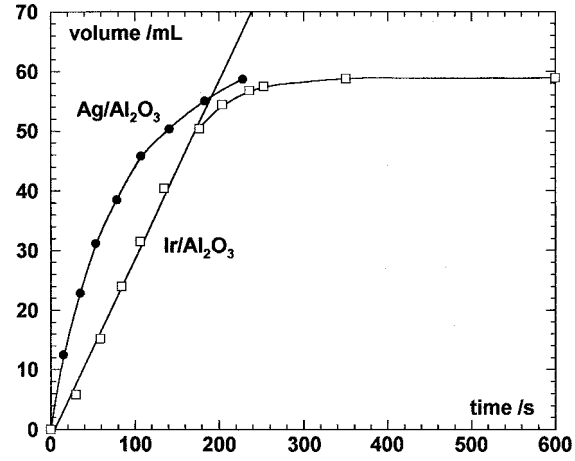

Fig. 2 Example of the two kinds of kinetics observed on curves $V(O_2)=f(t)$: Ir/Al_2O_3 catalyst, zero order (34 mg of grains, H_2O_2 1.62%) and Ag/Al_2O_3 catalyst, first order (40 mg of powder, H_2O_2 1.88%).

Results

Constant Pressure Reactor

With the constant pressure reactor, zero-order and first-order kinetics can be expected. Figure 2 shows measurements corresponding to both kinds of kinetic order.

The zero-order kinetics observed with the Ir/Al_2O_3 catalyst shows a linear increase of the oxygen volume vs time in Fig. 2. Then an important slope breaking follows after 85% decomposition due to concentration limitations. The final value is reached in an asymptotic way. The following equation gives the kinetic law:

$$2H_2O_2(aq) \rightarrow O_2(g) + 2H_2O(l) \quad (1)$$

$$v = \frac{d\xi}{dt} = \frac{dn(O_2)}{dt} = k_0[H_2O_2]^0 = k_0 \quad (2)$$

where

v = reaction rate, $mol \cdot s^{-1}$
ξ = extent of reaction, mol
t = time, s.
$n(O_2)$ = amount of released oxygen, mol
$[H_2O_2]$ = concentration of aqueous hydrogen peroxide, $mol \cdot l^{-1}$ or $mol \cdot ml^{-1}$
k_0 = zero-order rate constant, $mol \cdot s^{-1}$

It is possible to use directly the slope of the linear part of Fig. 2 to calculate the rate constant k_0.

Table 1 Results of kinetic studies

Sample	Shape	Mass, mg	$[H_2O_2]$, wt%	Order	k_1, ml · s^{-1}	k'_1, ml · s^{-1} · mg^{-1}	k_0, mol · s^{-1}	k'_0, mol · s^{-1} · mg^{-1}
Ag/Al_2O_3	Pellets	130	4.69	1	1.5×10^{-2}	1.2×10^{-4}	——	——
Ag/Al_2O_3	Pellets	187	4.69	1	1.1×10^{-2}	5.6×10^{-5}	——	——
Ag/Al_2O_3	Pellets	432	1.62	1	2.2×10^{-2}	5.1×10^{-5}	——	——
Ag/Al_2O_3	Powder	40	1.88	1	1.0×10^{-1}	2.5×10^{-3}	——	——
Ag/Al_2O_3	Powder	33	1.62	1	1.7×10^{-1}	5.6×10^{-3}	——	——
MnO_x/Al_2O_3	Powder	138	1.88	1	9.2×10^{-2}	6.7×10^{-4}	——	——
MnO_x/Al_2O_3	Powder	177	1.62	1	1.7×10^{-1}	9.4×10^{-4}	——	——
Pt/SiO_2	Grains	27	1.88	1	2.0×10^{-2}	7.5×10^{-4}	——	——
Pt/SiO_2	Powder	12	1.62	1	3.1×10^{-2}	2.5×10^{-3}	——	——
$Pt–Sn/Al_2O_3$	Powder	134	1.88	0	——	——	1.9×10^{-6}	1.4×10^{-8}
$Pt–Sn/Al_2O_3$	Powder	140	1.62	0	——	——	1.8×10^{-6}	1.3×10^{-8}
$Pt–Sn/Al_2O_3$	Powder	283	1.62	0	——	——	1.8×10^{-6}	0.6×10^{-8}
Ir/Al_2O_3	Grains	59	1.88	0	——	——	8.3×10^{-6}	14×10^{-8}
Ir/Al_2O_3	Grains	34	1.62	0	——	——	12×10^{-6}	35×10^{-8}
Ir/Al_2O_3	Powder	38	1.62	0	——	——	92×10^{-6}	240×10^{-8}

Table 2 Comparison of rate constants k'_0 for the catalysts leading to zero-order kinetics

Catalyst	k'_0/mol · s^{-1} · (mg catalyst)$^{-1}$	k'_0/mol · s^{-1} · (mg metal)$^{-1}$	k'_0/mol · s^{-1} · (mol metal)$^{-1}$
$Pt–Sn/Al_2O_3$ powder	$0.64–1.4 \times 10^{-8}$	$0.64–1.4 \times 10^{-6}$	$13–27 \times 10^{-2}$
Ir/Al_2O_3 grains	$14–35 \times 10^{-8}$	$0.39–0.97 \times 10^{-6}$	$7.5–19 \times 10^{-2}$
Ir/Al_2O_3 powder	240×10^{-8}	6.7×10^{-6}	130×10^{-2}

In the first-order kinetics case (Ag/Al_2O_3 catalyst, Fig. 2) a curvature is shown from the beginning of the reaction. The kinetic law can be written by using the following equations:

$$v = \frac{d\xi}{dt} = \frac{dn(O_2)}{dt} = -\frac{dn(H_2O_2)}{2\,dt} = \frac{V_s d[H_2O_2]}{2\,dt} = k_1[H_2O_2]^1 \quad (3)$$

where

$n(H_2O_2)$ = amount of hydrogen peroxide, mol
V_s = volume of H_2O_2 solution, ml
k_1 = first-order rate constant, ml · s^{-1}

The relationships for matter balance are

$$\xi = n_0(H_2O_2)/2 - n(H_2O_2)/2 = n(O_2) \quad (4)$$

where $n_0(H_2O_2)$ is the initial amount of hydrogen peroxide (mole).

At the end of the reaction,

$$n_0(H_2O_2)/2 = n_\infty(O_2) \quad (5)$$

where $n_\infty(O_2)$ is the maximum O_2 released (mole).

After integration of the initial relationship, we obtain the following relationships:

$$\ln[n(H_2O_2)/n_0(H_2O_2)] = -k_1 t/V_s \quad (6)$$

or

$$\ln\{[n_\infty(O_2) - n(O_2)]/n_\infty(O_2)\} = -k_1 t/V_s \quad (7)$$

For oxygen, the ratio of the numbers of moles is equal to the ratio of released volumes (measured in the same conditions, perfect gas assumption); therefore,

$$\ln\{[V_\infty(O_2) - V(O_2)]/V_\infty(O_2)\} = -k_1 t/V_s \quad (8)$$

or

$$\ln[1 - V(O_2)/V_\infty(O_2)] = -k_1 t/V_s \quad (9)$$

To check the order of the reaction, we have to solve

$$\ln[1 - V(O_2)/V_\infty(O_2)] = f(t) \quad (10)$$

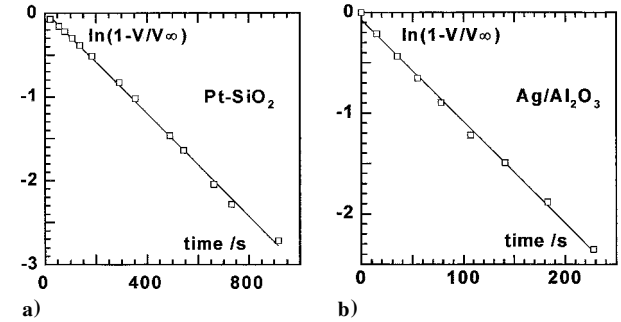

Fig. 3 Example of checking of the first order for two samples: a) Pt/SiO_2 catalyst (12 of mg powder, H_2O_2 1.62%) $k_1 = 3.1 \times 10^{-3}$ s^{-1}, where ——, is $y = 0.024714 - 0.0030611\,x$ and $R = 0.99922$ and b) Ag/Al_2O_3 catalyst (40 of mg powder, H_2O_2 1.88%), $k_1 = 1.0 \times 10^{-2}$ s^{-1}, where ——, is $y = 0.072259 - 0.010087\,x$ and $R = 0.99859$.

which must be a straight line going through the origin. Figure 3 gives the results corresponding to two first-order typical catalysts, Pt/SiO_2 and Ag/Al_2O_3.

The results obtained for the different samples studied are gathered in Table 1. To classify the samples, it is not possible to compare directly the rate constants, which correspond to different orders. Moreover, the loading of the active phase of the different catalysts is not the same. To overcome this, we have calculated specific or molar rate constant k' values corresponding to the mass (milligrams) of the sample or active phase or to the moles of the metal (Tables 2 and 3). The dispersion of the catalysts (number of surface metal atoms/total number of metal atoms) was not taken into account.

From Table 1, three main observations can be made from our experimental conditions: 1) the existence of zero-order and first-order reaction kinetics, depending on the nature of the catalyst; 2) the poor relationship between the rate constant and the mass of the catalyst; and 3) the importance of the sample shape. There is an increase of decomposition rate by a factor between 3 (Pt/SiO_2) and 100 (Ag/Al_2O_3) after grinding the pellets or grains.

The first observation can be roughly explained by a competition between adsorption and decomposition on the basis of the Langmuir isotherm[25]:

$$H_2O_2(aq) \underset{k_d}{\overset{k_a}{\rightleftharpoons}} H_2O_2(adsorbed) \quad (11)$$

Table 3 Comparison of rate constants k_1' for catalysts leading to first-order kinetics

Catalyst	k_1'/ml · s^{-1} (mg catalyst)$^{-1}$	k_1'/ml · s^{-1} (mg metal)$^{-1}$	k_1'/ml · s^{-1} · (mol metal)$^{-1}$
$[H_2O_2] = 4.69$ wt%			
Ag/Al_2O_3 pellets	$0.56–1.2 \times 10^{-4}$	$0.15–0.32 \times 10^{-2}$	160–340
$[H_2O_2] = 1.88$ wt%			
Ag/Al_2O_3 powder	2.5×10^{-4}	6.9×10^{-2}	7,400
MnO_x/Al_2O_3 powder	6.7×10^{-4}	4.1×10^{-2}	2,300
Pt/SiO_2 grains	7.5×10^{-4}	1.2×10^{-2}	2,300
$[H_2O_2] = 1.62$ wt%			
Ag/Al_2O_3 pellets	0.51×10^{-4}	0.14×10^{-2}	150
Ag/Al_2O_3 powder	56×10^{-4}	15×10^{-2}	16,000
MnO_x/Al_2O_3 powder	9.4×10^{-4}	5.9×10^{-2}	3,200
Pt/SiO_2 powder	25×10^{-4}	4.0×10^{-2}	7,800

Table 4 Comparison of V_{20} values for different samples[a]

Catalyst	V_{20}/ml · (mg catalyst)$^{-1}$	V_{20}/ml · (mg metal)$^{-1}$	V_{20}/ml · (mol metal)$^{-1}$
$[H_2O_2] = 4.69\%$			
Ag/Al_2O_3 pellets	$1.9 \times 10^{-2}–4.0 \times 10^{-2}$	0.51–1.1	$0.55 \times 10^5–1.2 \times 10^5$
$[H_2O_2] = 1.88\%$			
Ag/Al_2O_3 powder	35×10^{-2}	9.4	10×10^5
MnO_x/Al_2O_3 powder	9.2×10^{-2}	5.7	3.1×10^5
Pt/SiO_2 grains	10×10^{-2}	1.6	3.1×10^5
$Pt–Sn/Al_2O_3$ powder	0.65×10^{-2}	0.65	1.3×10^5
Ir/Al_2O_3 grains	6.6×10^{-2}	0.18	0.35×10^5
$[H_2O_2] = 1.62\%$			
Ag/Al_2O_3 pellets	0.6×10^{-2}	0.16	0.18×10^5
Ag/Al_2O_3 powder	66×10^{-2}	18	19×10^5
MnO_x/Al_2O_3 powder	1.1×10^{-2}	7.0	3.8×10^5
Pt/SiO_2 powder	30×10^{-2}	4.7	9.3×10^5
$Pt–Sn/Al_2O_3$ powder	0.65×10^{-2}	0.65	1.3×10^5
Ir/Al_2O_3 grains	16×10^{-2}	0.45	0.86×10^5
Ir/Al_2O_3 powder	120×10^{-2}	3.3	6.3×10^5

[a] O_2 volume obtained after 20 s reaction.

$$H_2O_2(\text{adsorbed}) \overset{k}{\rightleftharpoons} \tfrac{1}{2}O_2(g) + H_2O(l) \qquad (12)$$

where

k_a = adsorption rate constant
k_d = desorption rate constant
k = decomposition rate constant
K = equilibrium constant, k_a/k_d

If the rate is supposed to depend on the surface coverage θ, the following equation can be obtained:

$$v = k\theta = k(K[H_2O_2])/(1 + K[H_2O_2]) \qquad (13)$$

where v is the reaction rate (moles per second).

When the equilibrium constant K is high, that is, the adsorption rate is much higher than the desorption rate, we have $K[H_2O_2] \gg 1$ and

$$v = k \qquad (14)$$

Thus, we obtain a zero-order reaction kinetics.

When K is low so that $K[H_2O_2] \ll 1$, then

$$v = kK[H_2O_2] \qquad (15)$$

and the decomposition corresponds to a first-order reaction kinetics.

The real mechanism is much more complicated because the decomposition needs at least two H_2O_2 molecules and a part of the active phase centers can be blocked, depending on the catalyst mass, the H_2O_2 concentration, and the adsorption of oxygen. This can explain observation 2.

For the zero-order Ir/Al_2O_3 and $Pt–Sn/Al_2O_3$ catalysts, Table 2 gives the specific and molar activity results. The Ir/Al_2O_3 ground sample displays an activity nearly 10 times better than the grains. We can then classify the supported samples:

$$\text{Ir/(grains)} < \text{Pt–Sn/(powder)} < \text{Ir/(powder)}$$

First-order kinetics is observed for Ag/Al_2O_3, Pt/SiO_2, and MnO_x/Al_2O_3 catalysts (Table 3). The sample shape is of importance, powders always giving, as expected, much better performances than pellets: $k_1' = 0.15 \times 10^{-2}$ ml · s^{-1} · (mg Ag)$^{-1}$ for Ag/Al_2O_3 pellets and $k_1' = 15 \times 10^{-2}$ ml · s^{-1} · (mg Ag)$^{-1}$ for powder. For the same shape (powder, 0.1–0.25 mm) and the same H_2O_2 concentration, we can sort these catalysts as follows (k_1' expressed in milliliter per second per milligram metal):

$$Pt/SiO_2 < MnO_x/Al_2O_3 < Ag/Al_2O_3$$

To compare all of the samples, whatever the kinetic order, we have used the O_2 volume obtained after a fixed time, for example, 20 s contact time between H_2O_2 and catalyst (V_{20}). Table 4 gathers the V_{20} values for all of the samples. Using V_{20} values expressed in milliliters per milligram metal, for the same shape (powder, 0.1–0.25 mm) and the same H_2O_2 concentration (1.62 wt%), we can sort all the catalysts studied as follows:

$$Pt–Sn/Al_2O_3 < Ir/Al_2O_3 < Pt/SiO_2 < MnO_x/Al_2O_3 < Ag/Al_2O_3$$

Thus, even if other kinds of comparison are possible, we find again the two best classical catalysts used for propulsion.[9,15,17,26,27]

Constant Volume Batch Reactor

30 Percent H_2O_2

Table 5 gives a part of the results obtained on commercial silver catalysts (Ag and Ag/Al_2O_3), and Fig. 4 shows a comparison of both catalysts. As expected, the decomposition reaction starts at room temperature:

$$2H_2O_2(aq) \rightarrow 2H_2O(l \text{ or } g) + O_2(g) \qquad (16)$$

The activity of the supported catalyst is much higher in comparison to pure silver. This can be related to the higher specific surface

Table 5 Decomposition of 30 wt% H_2O_2 on silver catalysts (200 mg)[a]

Catalyst	Trial	Initial temperature, °C	Initial pressure, mbar	Final pressure, mbar	ΔP_{exp}, mbar	ΔP_{cale}, mbar
Ag	A	25	$<10^{-2}$	>100	>100	104
Ag/Al_2O_3	B	25	$<10^{-2}$	>100	>100	104
Ag/Al_2O_3	C	25	1020	1088	68	74
Ag/Al_2O_3	D	50	$<10^{-2}$	>180	>180	201

[a] Injection of 100 μl in evacuated reactor or at atmospheric pressure.

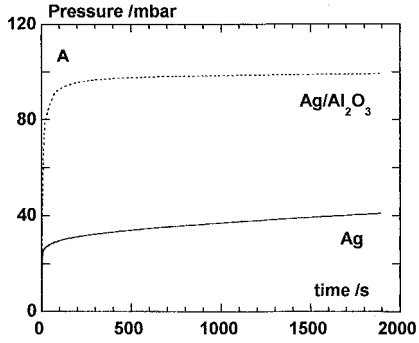

Fig. 4a Decomposition of H_2O_2 vs time on silver catalysts, initial temperature 25°C, injection 100-μl H_2O_2 30 wt% in evacuated reactor.

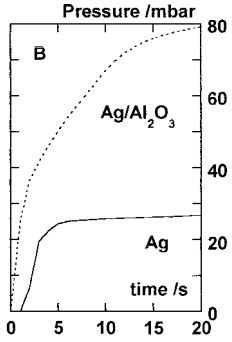

Fig. 4b Zoom of reaction onset.

area. The decomposition rate, as measured by the pressure increase, is rapid at the onset of the reaction: between 0 and 6 s the slopes are 9.6 and 6.5 mbar · s^{-1} and the decomposition delay is less than 1 and 2 s for the supported and the unsupported catalysts, respectively (Fig. 4b). After 10 s, the activity decreases strongly, leading to an approximately constant rate (0.24 mbar · s^{-1} for Ag/Al_2O_3 and 0.07 mbar · s^{-1} for Ag in the range of 10–20 s).

The pressure increase due to the evolved oxygen after 100 s is three times higher for the supported catalyst, approaching the calculated value for a whole decomposition (91 vs 104 mbar, Fig. 4a). After sufficient time (2000 s for supported catalyst vs 20,000 s for unsupported silver), the pressure increase reaches the calculated value in an asymptotic way (Table 5).

50 Percent H_2O_2

Figure 5 shows the results obtained for the same Ag/Al_2O_3 catalyst before and after grinding, for three successive injections of 50% H_2O_2 (100 μl). The initial pressure is about 1 bar argon, and the catalyst mass is 200 mg. The reactor pressure, the temperature of the catalyst, and the temperature of the gaseous atmosphere (not presented) have been simultaneously recorded, and the corresponding data are given in Table 6 for both silver samples and one manganese oxide catalyst. The first pressure step is always higher than the following ones because the saturation steam pressure has to be taken into account in addition to the released oxygen gas.

For both samples, the pressure steps match exactly the temperature peaks, and the zoom presented in Fig. 6 (for the manganese

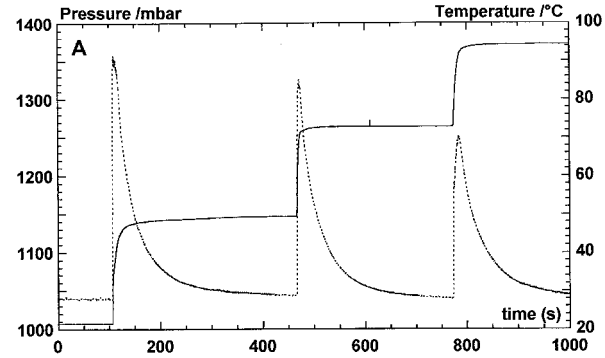

a) Grain catalyst

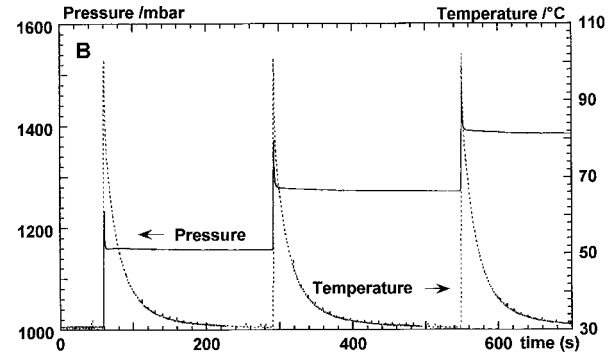

b) Milled catalyst

Fig. 5 Decomposition of 50% H_2O_2 on Ag/Al_2O_3 catalyst; variation of pressure and catalyst temperature vs time for 3 successive 100-μl injections from 1 bar argon pressure.

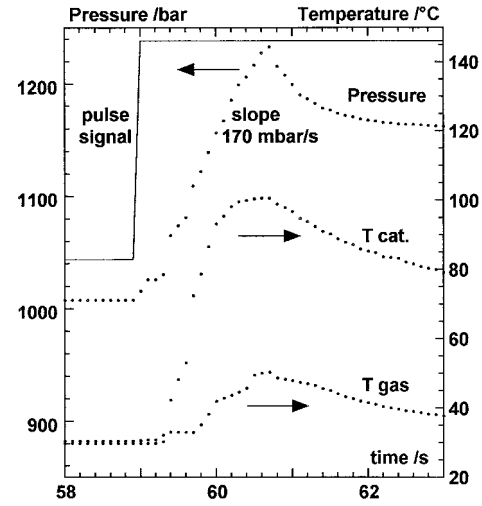

Fig. 6 Zoom of the first pulse for the decomposition of H_2O_2 on MnO_x/Al_2O_3 catalyst; data frequency 10 Hz for each gauge.

catalyst) shows that the temperature variations of the catalyst and the gas phase follow well the pressure changes at the time level of 0.1 s; therefore, they display the same decomposition delay (about 0.3 s for this case).

Comparison of Figs. 5a and 5b discloses different pressure profiles, with the ground Ag/Al_2O_3 sample displaying much better activity with sharp pressure peaks before the steps and thinner temperature peaks. The effect of sample grinding is to increase the reaction rate by more than one order of magnitude, in relation to the increase of the catalyst surface area. For the three injections, the temperature maximum corresponds to a small plateau at 101–104°C during about 0.5 s, in full agreement with the boiling of a part of the water. The grained catalyst shows a slight loss of activity evidenced by the decrease of the pressure slope, from 47 to 24 mbar · s^{-1}, in agreement

with the decrease of the maximal temperature of the catalyst from 91 to 70°C and the lower temperature reached by the gas (Table 6).

The catalytic activity of the supported manganese oxide sample is intermediate between the silver samples. The pressure slope is of the order of 200 mbar · s^{-1} and increases slightly with the injection number.

Effect of Stabilizing Agents

The influence on the catalytic activity of the addition of pyrophosphate $(P_2O_7)^{4-}$ ions is shown in Fig. 7 for Ag/Al_2O_3 and MnO_x/Al_2O_3 powdered samples. The lowest amount indicated on the curves corresponds to the commercial stabilizer loading. Both catalysts show an activity decrease as the amount of stabilizer increases. Moreover, the loss is much more drastic in the case of the MnO_x/Al_2O_3 sample. Thus, the decrease percentage calculated from the rate constants reaches 44% for the MnO_x/Al_2O_3 sample vs 31% for Ag/Al_2O_3. The (stabilizer)/(active center) molar ratios are in the range of 0.04–0.4. The important effect on MnOx-based catalysts can be explained by the transformation of the surface of manganese oxide into the more stable manganese phosphate or pyrophosphate.

Table 6 Decomposition of 50% H_2O_2[a]

Injection number	Pressure increase, mbar	Pressure slope, mbar · s^{-1}	Initial T, °C	T_{max} catalyst, °C	T_{max} gas, °C
		Ag/Al_2O_3, spheres			
1	138	47	28	91	29
2	117	36	28	85	29
3	108	24	28	70	29
		Ag/Al_2O_3 milled			
1	138	633	25	99	39
2	115	609	25	104	47
3	113	733	25	95	44
		MnO_x/Al_2O_3 powder			
1	152	170	30	101	50
2	121	196	30	102	50
3	118	212	30	103	48

[a] Successive pulses of 100 μl on three catalyst samples (200 mg).

However, the effect of stannate $(SnO_3^{2-}$ ions) addition appears completely different (Fig. 8). For the Ag/Al_2O_3 catalyst, we observed an increase of activities, whereas no influence occurred on the MnO_x/Al_2O_3 catalyst.

The influence of pyrophosphate on concentrated solutions was also studied for both catalysts, and the results are given in Tables 7 and 8. The sodium pyrophosphate was added to the 50 wt% H_2O_2 solution to obtain 1.0×10^{-4} mol · l^{-1} or 18 mg · l^{-1} of pyrophosphate anion. We can observe a limited influence of the pyrophosphate addition, but it must be noted that the catalyst is in excess [stabilizer/(active center) molar ratios in the range of $1.5–6 \times 10^{-4}$], and a real effect could be observed only after a sufficient number of H_2O_2 injections.

For the MnO_x/Al_2O_3 sample, a strong decrease of activity (measured by the pressure slope) is observed after three injections in the presence of pyrophosphate (Table 8), from 206 to 43 mbar · s^{-1}; these results are in full agreement with the results obtained with diluted hydrogen peroxide solutions.

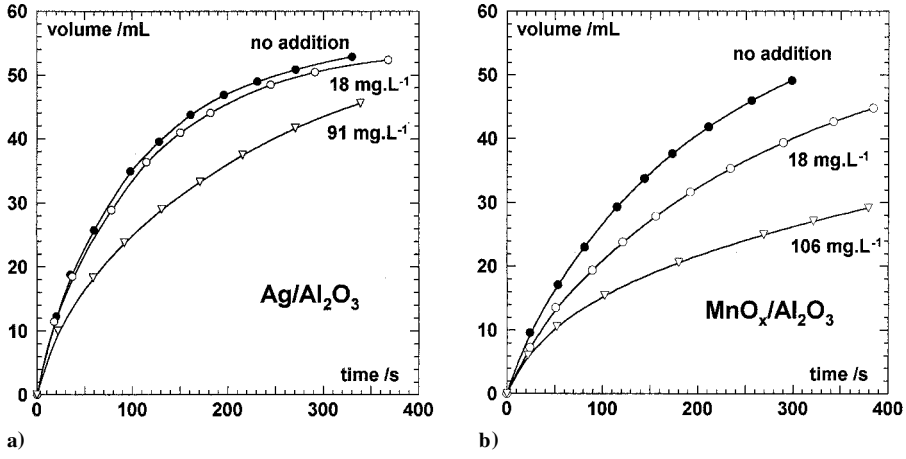

Fig. 7 Oxygen volume increase vs time for diluted H_2O_2 solutions (1.62 wt%) without and with addition of pyrophosphate ions (amounts indicated) a) for Ag/Al_2O_3 catalyst (powder, 36 mg) and b) for MnO_x/Al_2O_3 catalyst (powder, 86.5 mg).

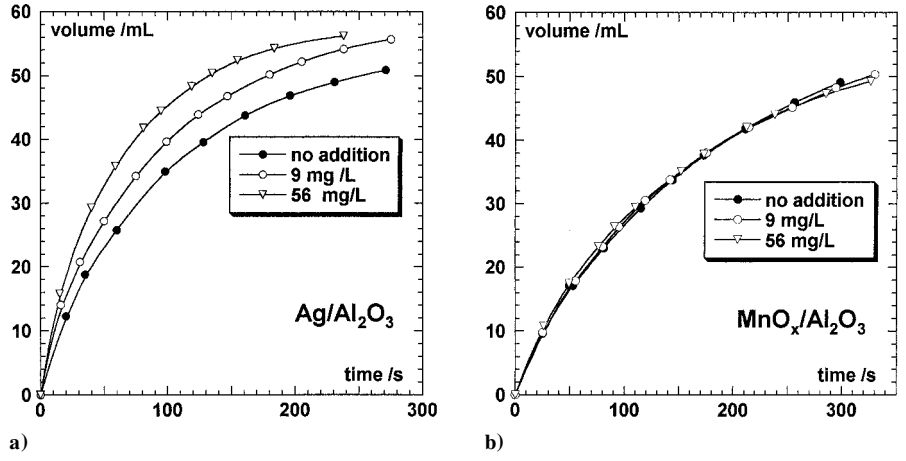

Fig. 8 Oxygen volume increase vs time for diluted H_2O_2 solutions (1.62 wt%) without and with addition of stannate ions (amounts indicated) a) for Ag/Al_2O_3 catalyst (powder, 36 mg) and b) for MnO_x/Al_2O_3 catalyst (powder, 86.5 mg).

Table 7 Results of decomposition of monopropellant 50% H_2O_2 without and with addition of pyrophosphate ions (18 mg · l^{-1}) on Ag/Al_2O_3 catalyst[a]

Injection number	Pressure increase, mbar	Pressure slope, mbar · s^{-1}	Initial T, °C	T_{max} catalyst, °C	T slope, °C · s^{-1}	T_{max} gas, °C
			H_2O_2 50%			
1	138	633	25	99	74	39
2	115	609	25	104	206	47
3	113	733	25	95	131	44
			H_2O_2 50% + $P_2O_7^{2(-)}$			
1	135	(99)	24	92	(40)	45
2	111	595	24	100	181	44
3	110	586	24	94	134	38

[a]Sieved powder (>0.08 mm), 200 mg, and successive 100-μl injections.

Table 8 Results of decomposition of monopropellant 50% H_2O_2 without and with addition of pyrophosphate ions (18 mg · l^{-1}) on MnO_x/Al_2O_3 catalyst[a]

Injection number	Pressure increase, mbar	Pressure slope, mbar · s^{-1}	Initial T, °C	T_{max} catalyst, °C	T slope, °C · s^{-1}	T_{max} gas, °C
			H_2O_2 50%			
1	152	170	30	101	72	50
2	121	196	30	102	61	50
3	118	212	30	103	57	48
			H_2O_2 50% + $P_2O_7^{2-}$			
1	135	206	23	101	53	33
2	110	149	23	96	49	35
3	112	43	23	93	21	25

[a]Powder, 200 mg, and successive 100-μL injections.

Conclusions

With the constant pressure reactor, the main results are 1) a first-order kinetics for Ag, Pt, and MnO_x active phases, whereas Ir and Pt–Sn gave zero-orderkinetics; 2) the sample shape is of importance, powders always giving much better performances than pellets; and 3) for the same samples shapes and the same H_2O_2 concentration, the increasing activity order is the following:

$$Pt\text{–}Sn/Al_2O_3 < Ir/Al_2O_3 < Pt/SiO_2 < MnO_x/Al_2O_3 < Ag/Al_2O_3$$

For both reactors, the addition of pyrophosphate ions leads to an activity decrease, mainly in the MnO_x supported sample case. The activity declines as the amount of stabilizers increases. Otherwise, the presence of stannate ions leads to a different behavior depending on the studied catalysts: no effect or a slight increase. To understand this peculiar behavior, more results are needed.

Acknowledgments

We thank the French Space Agency, Centre National d'Etudes Spatiales, Toulouse, for funding this study, S. Fouché and A. Melchior (SNECMA) for helpful discussions, and Ahmed Nohman (University of El-Minia, Egypt) for the design and realization of the constant pressure reactor.

References

[1]Schmidt, E., "Hydrazine and its Derivatives. Preparation, Properties, Applications," 2nd ed., Wiley, New York, 2001.

[2]Morgan, O. M., and Meinhardt, D. S., "Monopropellant Selection Criteria: Hydrazine and other Options," AIAA Paper 99-2595, June 1999.

[3]Meinhardt, D., Brewster, G., Christofferson, S., and Wucherer, E. J., "Development and Testing of New HAN-Based Monopropellants in Small Rocket Thrusters," AIAA Paper 98-4006, July 1998.

[4]Wuchere, E. J., Chistofferson, S., and Reed, B., "Assessment of High Performance HAN-monopropellants," AIAA Paper 2000-3872, July 2000.

[5]Meinhardt, D. S., Wucherer, E. J., Jankovsky, R. S., and Schmidt, E. W., "Selection of Alternate Fuels for Han-based Monopropellants," JANNAF Propellant Development and Characterization Subcommittee and Safety and Environmental Protection Subcommittee Joint Meeting, Vol. 1, April 1998, pp. 143–151.

[6]Meinhardt, D., Christofferson, S., and Wucherer, E. J., "Performance and Life Testing of Small HAN Thrusters," AIAA Paper 99-2881, June 1999.

[7]Anflo, K., Grönland, T. A., and Wingborg, N., "Development and Testing of ADN-Based Monopropellants in Small Rocket Engines," AIAA Paper 2000-3162, July 2000.

[8]Schöyer, H. F. R., Korting, P. A. O. G., Veltmans, W. H. M., Louwers, J., van der Heijden, A. E. D. M., Keizers, H. L. J., and v. d. Berg, R. P., "An Overview of the Development of HNF-Based Propellants," AIAA Paper 2000-3184, July 2000.

[9]Rusek, J., "New Decomposition Catalysts and Characterization Techniques for Rocket-Grade Hydrogen Peroxide," *Journal of Propulsion and Power*, Vol. 12, No. 3, 1996, pp. 574–579.

[10]Wernimont, E. J., and Mullens, P., "Recent Developments in Hydrogen Peroxide Monopropellant Devices," AIAA Paper 99-2741, June 1999.

[11]Long, M., and Rusek, J., "The Characterization of the Propulsive Decomposition of Hydrogen Peroxide," AIAA Paper 2000-3683, July 2000.

[12]Wernimont, E. J., and Meyer, S. E., "Hydrogen Peroxide Hybrid Rocket Engine Performance Investigation," AIAA Paper 94-3147, July 1994.

[13]Wernimont, E., and Garboden, G., "Experimentation with Hydrogen Peroxide Oxidized Rockets," AIAA Paper 99-2743, June 1999.

[14]Ventura, M., and Mullens, P., "The Use of Hydrogen Peroxide for Propulsion and Power," AIAA Paper 99-2880, June 1999.

[15]Morlan, P., Wu, P., Nejad, A., Ruttle, D., and Fuller, R., "Catalyst Development for Hydrogen Peroxide Rocket Engines," AIAA Paper 99-2740, June 1999.

[16]*Kirk-Othmer Encyclopoedia of Chemical Technology*, 4th ed., Vol. 13, Wiley, New York, 1995, pp. 961–995.

[17]Sellers, J. J., Brown, R., and Paul, M., "Practical Experience with Hydrogen Peroxide Catalysts," 1st International Hydrogen Peroxide Propulsion Conf., Univ. of Surrey and Surrey Space Center, Guildford, UK, June 1998.

[18]Ventura, M., and Garboden, G., "A Brief History of Concentrated Hydrogen Peroxide Uses," AIAA Paper 99-2739, June 1999.

[19]Eloirdi, R., Rossignol, S., Kappenstein, C., Duprez, D., and Pillet, N., "Design and Use of a Batch Reactor for Catalytic Decomposition of Different Mono-Propellants," AIAA Paper 2000-3553, July 2000.

[20]Eloirdi, R., Rossignol, S., Kappenstein, C., Duprez, D., and Pillet, N., "Monopropellant Decomposition Catalysts, Part 3: Design and Use of a Batch Reactor for Catalytic Decomposition of Different Propellants," *Journal of Propulsion and Power* (to be published).

[21]Bond, G. C., and Paal, Z., "Recently Published Work on Europt-1, a 6.3% Pt/SiO_2 Reference Catalyst," *Applied Catalysis A*, Vol. 86, 1992, pp. 1–35.

[22]El Abed, A., El Qebbaj, S. E., Guérin, M., Kappenstein, C., Dexpert, H., and Villain, F., "In Situ EXAFS Studies of $Pt\text{-}Sn/Al_2O_3$ Catalysts Prepared by a New Procedure," *Journal de Chimie Physique*, Vol. 94, 1997, pp. 54–76.

[23]Kappenstein, C., Guérin, M., Lazar, K., Matusek, K., and Paal, Z., "Characterization and Activity in n-Hexane Rearrangement Reactions of Metallic Phases on $Pt\text{-}Sn/Al_2O_3$ Catalysts of Different Preparations," *Journal of the Chemical Society, Faraday Transactions*, Vol. 94, No. 16, 1998, pp. 2463–2473.

[24]Kappenstein, C., Wahdan, T., Duprez, D., Zaki, M. I., Brands, D., Poels, E., and Bliek, A., "Permanganic Acid: A Novel Precursor for the Preparation of Manganese Oxide Catalysts," *Proceedings of the Sixth International Symposium on the Preparation of Catalysts*, Louvain la Neuve, B, Sept. 1994, in Studies in Surface Science and Catalysis, Vol. 91, 1995, pp. 699–706.

[25]Atkins, P. W., *Physical Chemistry*, 6th ed., Oxford Univ. Press, Oxford, 1998, pp. 761–792.

[26]Pourpoint, T. L., and Rusek, J. J., "Investigation of Homogeneous and Heterogeneous Catalysis for the Propulsive Decomposition of Hydrogen Peroxide," 1st International Conf. on Green Propellants for Space Propulsion, ESA–European Space Research and Technology Center, June 2001.

[27]Yang, H., Zhang, T., Tian, H., Tang, J., Xu, D., Ren, L., Zhao, J., and Lin, L., "Perowskite-Type Oxides: A Novel Type of Catalysts Suitable for Hydrogen Peroxide Decomposition," 1st International Conf. on Green Propellants for Space Propulsion, ESA–European Space Research and Technology Center, June 2001.